

## LANDSAT IMAGE PROCESSING AND CLASSIFICATION IN IDRISI SELVA

*Макалада IDRISI Selva программасындагы спутник Landsat аркылуу көрүнүүчү негизги кадамдагы окшоштуктар каралат, тагыраак айтканда, текшерилүүчү же текшерилбөөчү ыкмалардын жардамы менен кийинки территориянын классификациясы үчүн шоола энергиясын иштетип, көрсөтүүнүн сапаты жакшыртылат.*

*В статье рассматривается аналогия основных шагов обработки спутниковых изображений Landsat в программе IDRISI Selva, а именно радиометрическая обработка, позволяющая улучшить качество изображений для дальнейшей классификации территории с помощью контролируемых и неконтролируемых методов классификаций.*

*The article covers main steps analogy of Landsat satellite image processing in IDRISI Selva that is radiometric calibration permits to enhance quality of images for further territory classification with supervised and unsupervised methods of classification.*

Remote sensing can be broadly defined as the collection and interpretation of information about an object, area, or event without being in physical contact with the object. Aircraft and satellites are the common platforms for remote sensing of the earth and its natural resources. Aerial photography in the visible portion of the electromagnetic wavelength was the original form of remote sensing but technological developments has enabled the acquisition of information at other wavelengths including **near infrared, thermal infrared and microwave**. Collection of information over a large numbers of wavelength bands is referred to as multispectral or hyper spectral data. The development and deployment of manned and unmanned satellites has enhanced the collection of remotely sensed data and offers an inexpensive way to obtain information over large areas. The capacity of remote sensing to identify and monitor land surfaces and environmental conditions has expanded greatly over the last few years and remotely sensed data will be an essential tool in natural resource management /3/.

There are many electromagnetic (EM) band-length ranges Earth's atmosphere absorbs. The EM band ranges transmittable through Earth's atmosphere are sometimes referred to as atmospheric windows. The human eye only detects, viz. the reflective solar radiance humans actually see, that part of the EM scale in the band length range 0.4 – 0.7  $\mu\text{m}$ . But remote sensing technology allows for the detection of other reflective and radiant (e.g. thermal) energy band-length ranges that reach or are emitted by Earth's surface, and even some Earth's atmosphere reflects, e.g. the EM reflective qualities of clouds. Hence, for viewing purposes red, green, and blue (RGB) false color assignments are used to express the reflective qualities of objects in these EM band-length groups, and the combination and mixing of these false color assignments express the true physical reflective qualities of all objects present in an image /6/.

Present work based on the scene of LANDSAT ETM+ product ordered from USGS GloVis: The Global Visualization Viewer. Nowadays all LADSAT data available in USGS archive and can be freely obtained from three USGS websites. The USGS GloVis Viewer contains an interactive map to search for data by entering the geographic coordinates (latitude and longitude) or path and row of required satellite image.

Obtained satellite image covers Naryn region - 149 Path and 31 Row (Figure 1).

Figure 1. USGS GloVis view window

USGS GloVis contains Landsat archive up to date from different sensor types. For this research was used the scene from Landsat ETM+ sensor type for August, 2009. To better examine and analyze dataset has cloud coverage less than 10%. All Landsat data orthorectified and provided in different formats. In this case GeoTIFF format dataset was used.

Landsat images have a radiometric resolution of eight bits, which means DN values range of 0 – 255. The Table below describes characteristics of LANDSAT ETM+ sensors. Landsat has spatial resolution of 30 m at nadir.

Table 1. Sensor specifications

| Sensor Characteristics | IFOV   | Spectral Bands   | Swath Width | Radiometric resolution | Repeat Cycle |
|------------------------|--|--|-------------|------------------------|--------------|
| Landsat ETM+           | 30 meters (Bands 1-5, 7)<br>120 meters (Band 6)<br>30 meters (PAN) | <ul style="list-style-type: none"> <li>0.45 - 0.515 (um)</li> <li>0.55 - 0.605 (um)</li> <li>0.63 - 0.69 (um)</li> <li>0.7 - 0.90 (um)</li> <li>1.1 - 1.25 (um)</li> <li>1.65 - 1.75 (um)</li> <li>2.13 - 2.35 (um)</li> <li>10.40 - 12.5 (um)</li> <li>Band 8: 0.52 - 0.9 (um)</li> </ul> | 183 km      |                        | 16 days      |

Landsat images come in many different formats. GeoTIFF Landsat image came with eight bands where Bands 1-5, 7 are reflective, Band 6 is thermal and Band 8 is panchromatic band.

For radiometric enhancement and further image processes, we used reflective bands only. IDRISI Selva is an integrated GIS and Image Processing software solution and provides nearly 300 modules for the analysis and display of digital spatial information.

IDRISI supports raster images in actual data file, which has an “.rst” file extension.

Before analyze the data it's needed to perform some pre-processing to normalize data (to allow quantitative comparison between images) and remove atmospheric effects. To enhance data quality applied radiometric calibration. Calibration steps in IDRISI were performed by Image Calculator from Modeling Menu by the following equations.

*Conversion to at-sensor spectral radiance ( $Q_{cal-to-L_\lambda}$ )*

Calculation of at-sensor spectral radiance is the fundamental step in converting image data into a meaningful common radiometric scale. During radiometric calibration, pixel values are converted to units of absolute spectral radiance using 32-bit floating-point calculations. The following equation is used to perform the  $Q_{cal-to-L_\lambda}$  conversion:

$$L_\lambda = \left( \frac{LMAX_\lambda - LMIN_\lambda}{Q_{calc\ max} - Q_{calc\ min}} \right) (Q_{cal} - Q_{cal\ min}) + LMIN_\lambda$$

where,

$L_\lambda$  – Spectral radiance at the sensor's aperture [ $W/(m^2sr\ \mu m)$ ];

$Q_{cal}$  – Quantized calibrated pixel value [DN];

$Q_{cal\ max}$  and  $Q_{cal\ min}$  – Maximum and minimum quantized calibrated pixel value corresponding to  $LMAX_\lambda$  and  $LMIN_\lambda$  respectively [DN];

$LMIN_\lambda$  and  $LMAX_\lambda$  - Spectral at-sensor radiance that is scaled to  $Q_{cal\ min}$  and  $Q_{cal\ max}$  respectively [ $W/(m^2\ sr\ \mu m)$ ];

*Conversion to TOA reflectance ( $L_\lambda-to-\rho_p$ )*

A reduction in scene-to scene variability can be achieved by converting the at-sensor spectral reflectance to exoatmospheric TOA reflectance, also known as in-band planetary albedo.

When comparing images from different sensors, there are three advantages to using TOA instead of at-sensor spectral radiance. First is removes the cosine effect of different solar zenith angles due to the time difference between data acquisitions. Second, TOA reflectance compensates for different values of the exoatmospheric solar irradiance arising from spectral band differences. Third, the TOA reflectance corrects for the variation in the Earth-Sun distance between different data acquisition dates. These variations can be significant geographically and temporally. The TOA reflectance of the Earth is computed according to the below equation /1/:

$$\rho_{\lambda} = \frac{\pi \cdot L_{\lambda} \cdot d^2}{ESUN_{\lambda} \cdot \cos \theta_s}$$

where,

$\rho_{\lambda}$  – Planetary TOA reflectance [unitless];

$\pi$  – Mathematical constant equal to 3.14159 [unitless];

$L_{\lambda}$  - Spectral radiance at the sensor's aperture [ $W/(m^2 sr \mu m)$ ];

$d$  – Earth-Sun distance [astronomical units];

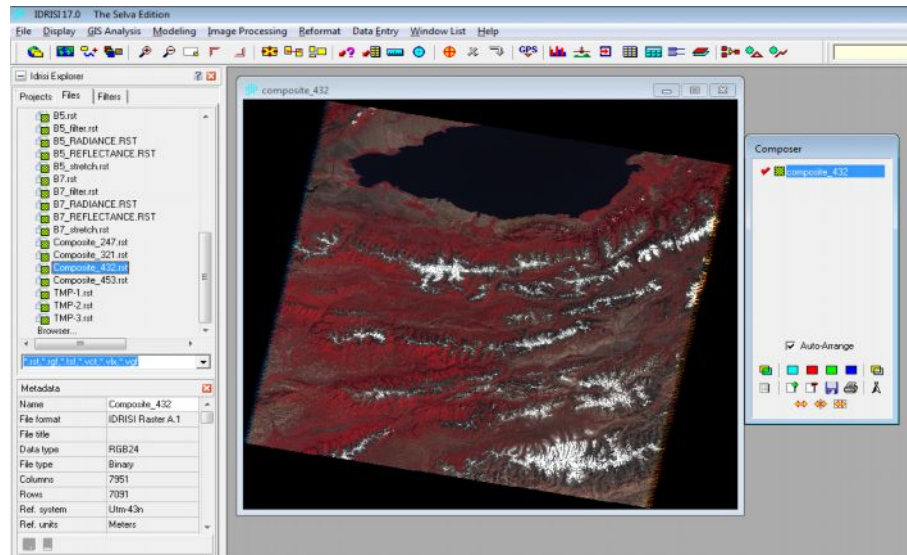
$ESUN_{\lambda}$  – Mean exoatmospheric solar irradiance [ $W/(m^2 \mu m)$ ];

$\theta_s$  – Solar zenith angle [degrees]

Radiance and reflectance for each band were calculated by using above described equations. Required parameters were taken from Metafile (.MTL) which is given for each Landsat image.

To blur image and remove noise Gaussian Filtering with  $3 \times 3$  kernel size applied to all bands 1-5 and 7. Gaussian filter is commonly used to generalize image. The output value is the sum of the products of each pixel value and its corresponding kernel value. After correction all bands were stretched by using Image Processing Enhancement Module specified lower band as 0 thus remove no data pixels. Stretch provides methods for rescaling image values to a new range of value. In this case simple linear equalization was applied.

Figure 2. False Color Composition of Landsat image



Most earth observation satellites record in several spectral bands, in other words the satellite records a number of small wavelength intervals within the electromagnetic spectrum (visible light, near and short wave infrared). By means of the basic colours red, green and blue (RGB) it is possible to construct several band combinations in which the colours tell something about the parts of the spectrum that are represented in RGB /4/.

The image classification process involves conversion of multi-band raster imagery into a single-band raster with a number of categorical classes that relate to different types of land cover /2/.

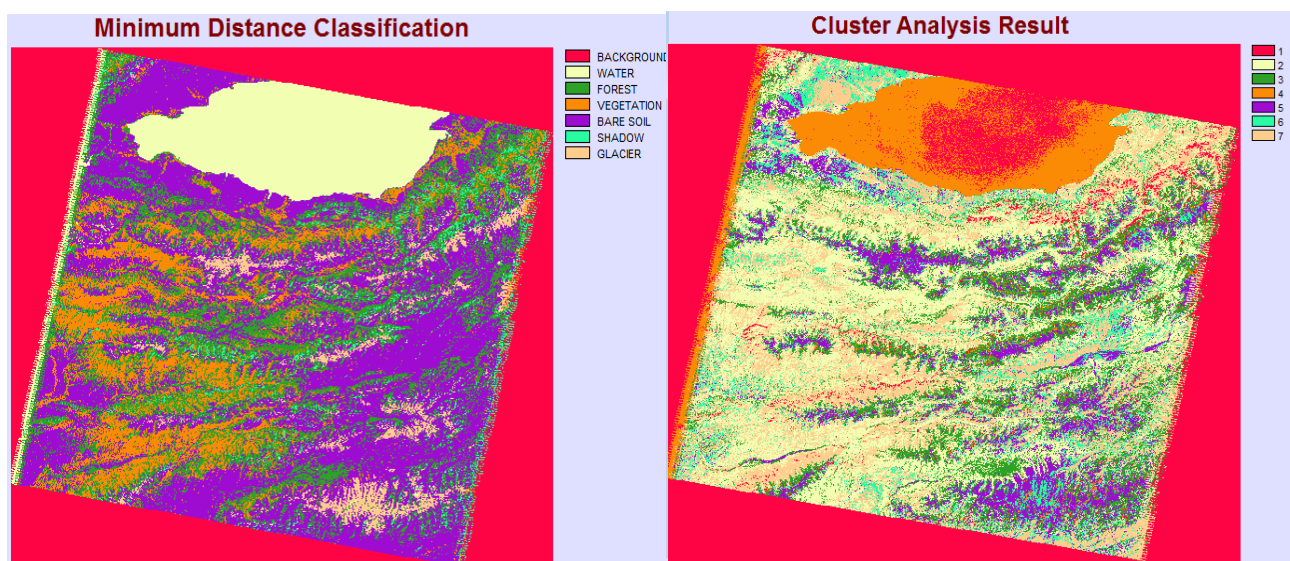
Before classification there were acquired signatures for each cover class by digitizing homogenous areas (group of pixels) subsequently, enable the program to match unknown pixels with alike reflectance to one (known) training site signature. The areas selected to serve, as training sites should be relatively homogeneous and extensive enough to provide good statistics. The LANDSAT image was classified into seven classes: 1 - background, 2 - water, 3 - forest, 4 - vegetation, 5 - bare soil, 6 - shadow and 7 - glacier (Figure 3).

Typically, background and shadows are not separated into individual layers. Here, it was done to distinguish water body against background and shadows. Due to mountain environment some areas faces North aspect forming then shades. Water and shadows have almost the same reflectance thus during classification process all pixels similized in a single class.

Once the training sites signature files were developed the classification methods' are applied at later stage. There are two common ways to classify satellite images: supervised and unsupervised classifications. The classification process may be supervised when it uses training samples to learn the spectral characteristics of the informational classes, or unsupervised if the supply of training samples is impossible or severely limited. By checking the emission value of every pixel, images can be classified and spectral character determined. The Minimum Distance Classification (MINDIST) and CLUSTER classifiers are among of the most advanced classification method used in this work.

With the minimum distance to class means classifier algorithm data is used only to determine class means. The MINDIST classification is based on the mean reflectance on each band for a signature. Classification is then performed by placing a pixel in the class of the nearest mean. MINDIST is commonly applied when the number of pixels used to define signatures is very small or when training sites are not well defined.

CLUSTER provides an unsupervised classification of input images using histogram peak technique. The spectral information from used different bands computes to an index number in and internally produces 3-dimensional histograms for all bands used. Classes are identified as histogram 'peaks' (centers of high frequency). Membership to a class is defined by the neighborhood to such 'peak' /5/. For our Landsat ETM+ maximum option for 10 clusters was selected because more than 10 classes is not realistic for Landsat classification in mountains environment due to of 30 m spatial resolution. Figure 3 ((a) and b)) below shows applied image classification techniques.



The IDRISI Selva CLUSTER algorithm was set to fine classification and a user-defined number of classes with all the other settings at the default position. During the first step of CLUSTER classification, there were selected 10 classes and then reclassified with RECLASS algorithm to show the main mentioned six land use categories.

The purpose of this classification processes was to learn principles of supervised and unsupervised methods. As using Landsat 30 meters spatial resolution image for this purpose there was no reason to differentiate more classes. Moreover, close distance between classes, hilly area, different aspects and various types of soil, all three categories represent mixed pixels that influents on classification.

The FISHER classifier conducts a linear discriminant analysis of the training site data to form a set of linear functions that express the degree of support for each class. The assigned class for each pixel is that class which receives the highest support after evaluation of all functions. These functions have a form similar to that of a multivariate linear regression equation, where the independent variables are the image bands, and the dependent variable is the measure of support. In fact, the equations are calculated such that they maximize the variance between classes and minimize the variance within classes. The number of equations will be equal to the number of classes, each describing a hyperplane of support. The intersections of these planes then form the boundaries between classes in band space.

KNN classifier assumes that pixels close to each other in spectral space are likely to belong to the same class. In its simplest form, an unknown pixel is labeled by examining the available training pixels in the spectral domain and choosing the class most represented among a pre-specified number of nearest neighbors. The comparison essentially requires the distances from the unknown pixel to all training pixels to be computed.

Figure 4 shows classification by FISHER module and K-nearest neighborhood (KNN) classifier.

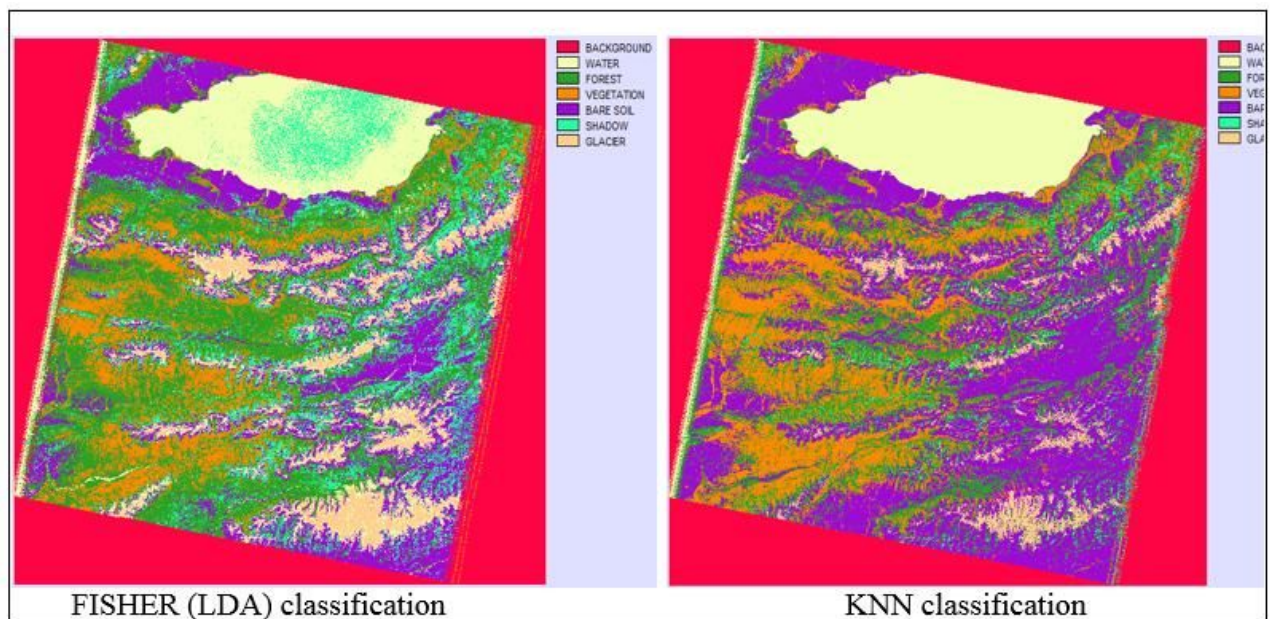


Figure 4. a) FISHER (LDA) classification, b) KNN classification

All classified images were analyzed using the AREA algorithm (Table 2 and Figure 5).

Table 2. Area of defined land use classes by different classifiers

| Class      | AREA, sq. km |            |           |            |
|------------|--------------|------------|-----------|------------|
|            | MINDIST      | FISHER     | KNN       | CLUSTER    |
| Water      | 4972.9806    | 6004.2681  | 4980.7035 | 10292.4828 |
| Forest     | 8673.1065    | 10674.0657 | 8107.5861 | 5208.4161  |
| Vegetation | 4890.9132    | 4386.4218  | 6583.6089 | 4087.1655  |

|                   |                 |           |            |           |
|-------------------|-----------------|-----------|------------|-----------|
| Bare soil         | 15415.2684      | 7804.4967 | 14314.9257 | 3569.2758 |
| Shadow            | 996.5079        | 4906.0305 | 942.0804   | 3074.1408 |
| Glacier           | 1396.2906       | 1962.1998 | 1422.4626  | 8179.5087 |
| <b>Total area</b> | <b>50742.49</b> |           |            |           |

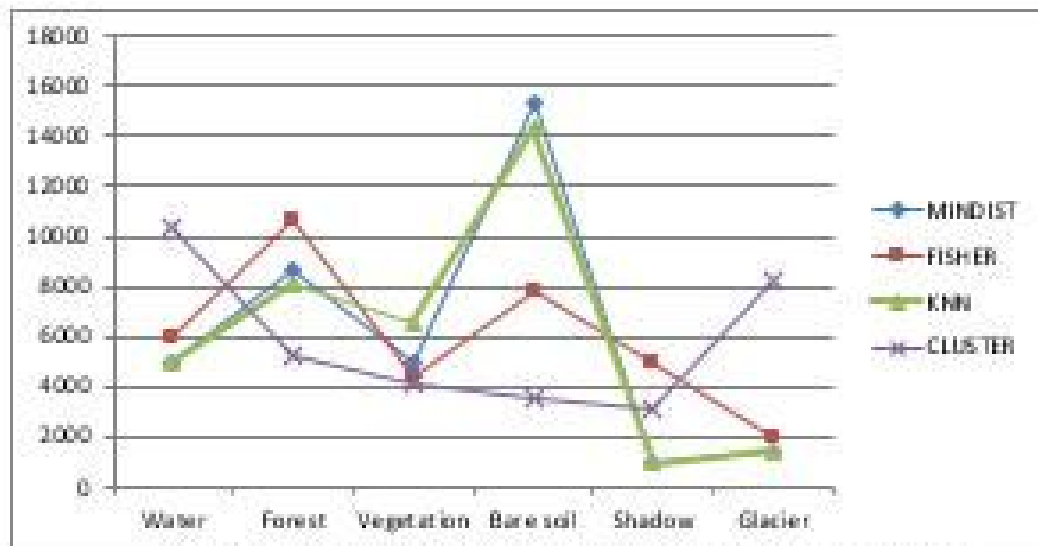


Figure 5. Area of defined land use classes by different classifiers

All methods used in this work are hard classifiers, which means that they assign each pixel to a fixed class.

The accurate land cover area calculation in Tian-Shan environment is quite difficult due to complex landscape and abandonment of land.

According to CLUSTER unsupervised classification most of the study area is covered by water surface and glaciers. Most of the time during the year this is covered by fresh snow and glaciers, but considering the season of token image this result is typically wrong. On the other hand, the unsupervised cluster classification is a very quick way to gain knowledge of the study area. Unsupervised classification process yields new information that the analyst may use in further process. To acquire more precise land cover map fieldwork of case study is required too.

MINDIST and KNN classification seems cover training sites in almost similar proportions.

The land use categories “Fosrest” and “Vegetation” were difficult to separate from each other. Vegetation in summer season varies from very bright green-to-green color. Some pixels were token to “Forest” class due to wetness of ground. So resulting these two classes were not clearly separated by all algorithms.

## References

1. Gyanesh Chander, Brian L. Markham, Dennis L. Helder (2009). Summary of current radiometric calibration for Landsat MSS, TM, ETM+ and EO-1 ALI sensors. Remote Sensing of Environment 113 (2009) 893-903
2. <http://blogs.esri.com/esri/arcgis/2011/05/28/classifying-landsat-image-services-to-make-a-land-cover-map/>

g.pdf

3. [ftp://ftp.wsl.ch/downloads/babst/Fernerkundung\\_WS2012/literatur/remote\\_sensin](ftp://ftp.wsl.ch/downloads/babst/Fernerkundung_WS2012/literatur/remote_sensin)
4. [http://gdsc.nlr.nl/gdsc/en/information/earth\\_observation/band\\_combinations](http://gdsc.nlr.nl/gdsc/en/information/earth_observation/band_combinations)
5. <http://uhaweb.hartford.edu/gatetutor/idrisi/improc5a.html>
6. [http://www.yale.edu/gsp/gis-files/remote\\_sensing\\_intro.pdf](http://www.yale.edu/gsp/gis-files/remote_sensing_intro.pdf)